Indonesian Geotechnical Journal, August 2022, Vol 1 (2). Page 1-11
DOI: https://doi.org/10.56144/igj.v1i2.10
EISSN 2829-7520
https://indonesian-geotechnical-journal.org/index.php/JGI/issue/archive

Lower Bound Capacity of Strip Footings on Rock Masses with Two Discontinuity Sets

Widjojo Adi Prakoso[1,*]
[1]Department of Civil and Environmental Engineering, Universitas Indonesia, Depok 16424, Indonesia; wprakoso@eng.ui.ac.id
*Correspondence: wprakoso@eng.ui.ac.id

SUBMITTED 23 May 2022 **REVISED** 04 June 2022 **ACCEPTED** 06 June 2022

ABSTRACT This study presents a lower bound model for predicting the strip footing bearing capacity on rock masses with two sets of ubiquitous closed discontinuities. The model explicitly considers the intact rock's strength and the discontinuities, as well as its number and orientation. The model validation was presented. The parametric study of footings on rock masses with two discontinuity sets having the same strength was performed, and the results were graphically reported in detail. It was observed that the bearing capacity was controlled primarily by the rock structures, such as the discontinuity sets and orientation, as well as the discontinuity strength. It is also controlled by the intact rock strength for a very limited number of cases. The minimum bearing capacity factor is independent of the intact rock friction angle, but it is a linear function of discontinuity cohesion. Furthermore, it is expressed in relation to UCS, in which the ratio for the maximum bearing capacity was insignificantly affected by intact rock friction angle, and not linearly correlated to discontinuity cohesion. This bearing capacity factor for rock masses with low discontinuity strengths tends to be more sensitive to variations in discontinuity orientation. The exception to the above points are that some rock mass conditions would lead to unexpected rock footing bearing capacities, indicating that good characterization processes of rock masses are always essential. Subsequently, the practical significance of this study was briefly discussed.

KEYWORDS Rock footings; Rock masses; Bearing capacity; Discontinuity orientation; Discontinuity strength

1 INTRODUCTION

Strip footings are often the first selection when designing foundations on rock masses, and one of the design criteria is whether the rock mass is able to resist the imposed bearing pressure. This simply means that there is a need to analyze the rock footing bearing capacity, which is typically determined using empirical formulas or even prescribed values (e.g., Goodman, 1980), because of the difficulty in deriving the theoretical bearing capacity. This challenge primarily arises from the inability to properly characterize the rock mass structures and conditions such as discontinuity number, orientation, and strength. Despite this challenge, theoretical solutions were still developed for footings on rock masses with implicit discontinuities (e.g., Merifield *et al.*, 2006 & Chakraborty and Kumar, 2015). Prakoso and Kulhawy (2004a) proposed the theoretical solutions for strip footings on rock masses with explicit sets of ubiquitous closed discontinuities, and further extend this study with "nominally open" vertical discontinuities (Prakoso and Kulhawy, 2006). Prakoso and Kulhawy (2006, 2011) performed Monte Carlo simulations and found that the variability of intact rock strength does not significantly affect the footing bearing capacity. The importance of rock discontinuities has also been reported by Prakoso and Kulhawy (2004b).

This present study is an extension of the lower bound models for rock foundations proposed by Prakoso and Kulhawy (2004a), and it presents the bearing capacity of strip footings on rock masses with two sets of ubiquitous closed discontinuities. The model explicitly considers the strength of the intact rock and the discontinuities, as well as its number and orientation. Furthermore, a synthesis of general practical trends of the bearing capacity factor is to be highlighted.

2 LOWER BOUND BEARING CAPACITY MODEL

Prakoso and Kulhawy (2004a) proposed a conservative lower bound bearing capacity model for strip foundations generally known as the Bell model (Bell, 1915), coupled with a simple discontinuity strength as shown in Figure 1a. This model assumes inherently that the discontinuity spacing is small relative to the mobilized rock mass, and therefore the discontinuity spacing is not considered explicitly in the model. The overall approach can be easily performed manually or implemented in a spreadsheet program, and therefore may serve as a more rational alternative to arbitrarily prescribed values in many building codes.

The lower bound bearing capacity of a strip footing on a rock mass surface is presented in the following format:

$$q_{ult} = c_r \cdot N_{cs} \tag{1}$$

Where c_r = rock material cohesion and N_{cs} = bearing capacity factor. The rock mass weight affected by the footing is insignificant when compared to c_r, hence, it is not taken into account in the model. The consequences of this assumption were that the footing width and its embedment depth do not significantly affect the bearing capacity (Galindo *et al.*, 2017). The strength of the rock material and the discontinuities follow the Mohr-Coulomb criterion. The criterion used is admittedly a simplified approach, but it helps to have a consistent strength criterion for both the rock material and the discontinuities. Furthermore, the values used in this criterion could be derived from linearization processes of more advanced strength criteria for both the rock material and the discontinuities (e.g., Hoek, 2007).

The shear strength of the rock material is given by:

$$\tau_r = c_r + \sigma \tan \phi_r \tag{2}$$

Where ϕ_r = rock material friction angle, and the shear strength along the i-th discontinuity set having an orientation angle of θ to the horizontal plane as shown in Figure 1 is expressed as follows:

$$\tau_{ji} = c_{ji} + \sigma \tan \phi_{ji} \tag{3}$$

In which c_{ji} and ϕ_{ji} are discontinuity cohesion and friction angle of the i-th discontinuity set, respectively. Meanwhile, the discontinuity has no tensile strength.

The Bell model for a rock mass with two discontinuity sets is shown schematically in Figure 1b. The two discontinuity sets have orientation angles of θ_1 and θ_2 (= $\theta_1 + \Delta_\theta$, less than 180°). The method proposed by Prakoso and Kulhawy (2004a) is extended to two discontinuity sets with different strengths as detailed in the appendix.

The results of this current model in terms of N_{cs}, were validated against those developed by Sutcliffe *et al*. (2004). The bearing capacity factor for strip footings on rock masses with two discontinuity sets (Δ_θ = 15º, 45º, and 75º and same discontinuity strength parameters) was compared with that of Sutcliffe *et al*. (2004) as shown in Figure 2. It is noted that the results reported by Sutcliffe *et al*. (2004) have been further validated by Salari-Rad *et al*. (2013), in which two different sets of discontinuity strength parameters were considered for each Δ_θ value. Similar to the findings discussed in Prakoso and Kulhawy (2004), N_{cs} based on the current model was lower than that based on the other models, but the trend of N_{cs} variation with discontinuity orientation angle θ_1 was similar for all parameter combinations. Based on the six combinations shown, the difference in N_{cs} between the two models depends on different rock mass parameters including discontinuity strength and orientation parameters. This validation process complements the one performed by Prakoso and Kulhawy (2004a) for strip footings on rock masses with one and two discontinuity sets (Δ_θ = 90º and the same discontinuity strength parameters) with those from plasticity and finite element models reported by Davis (1980), Booker (1991), Alehossein *et al.* (1992), and Yu and Sloan (1994).

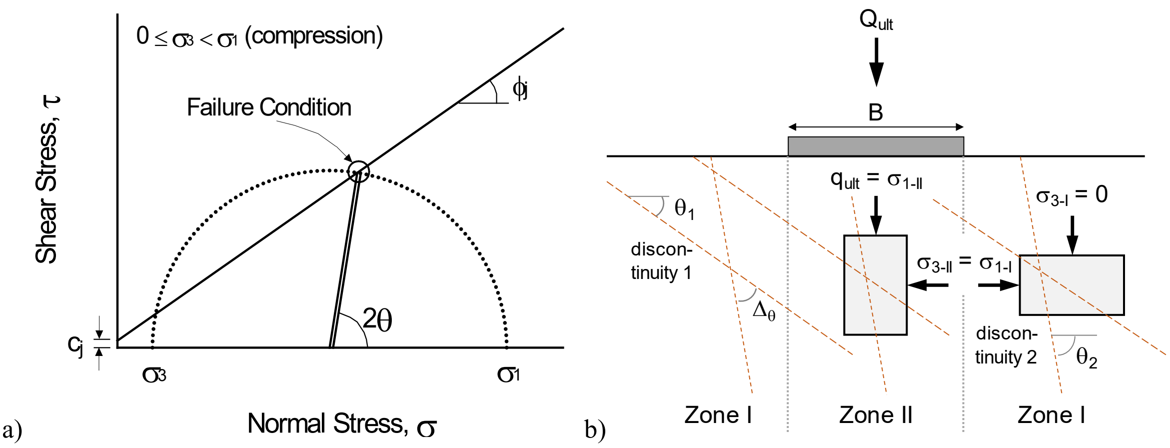

Figure 1. Assumptions: a) State of stress at failure for discontinuities, and b) lower bound capacity model for rock masses with one discontinuity set (modified after Prakoso and Kulhawy, 2004a).

3 PARAMETRIC STUDY

This is a parametric study for rock masses with two discontinuity sets that has similar strengths, even though the model is able to analyze different discontinuity strengths. For a reference, the values of N_{cs} for intact rock with ϕ_r = 30º, 35º, 40º, and 45º are 13.8, 18.0, 24.0, and 32.9, respectively. The lower bound bearing capacity was also expressed in terms of its ratio to the intact rock uniaxial compressive strength (q_{ult}/UCS), hence, the ratios for the above ϕ_r values are 4.00, 4.69, 5.60, and 6.83, respectively.

Three Δ_θ values were considered, and Figures 3, 4, and 5 show the results for Δ_θ = 90º, 60º, and 30º, respectively. The general shape of N_{cs} curve, for any combination of discontinuity friction angle ϕ_j and discontinuity cohesion c_j/c_r, is different for rock masses having varying Δ_θ values, indicating a significant effect of the discontinuity orientation properties on rock footing bearing capacity.

The general shape of N_{cs} curves for Δ_θ = 90º in Figures 3a through 3d is similar, relatively independent of combination of ϕ_j and c_j/c_r. Figures 3a and 3b suggest that, for rock masses with relatively low discontinuity shear strength, N_{cs} (= 13.8 – 32.9) is controlled by the intact rock strength for only very narrow ranges of discontinuity orientation angle θ_1 (θ_1 < 2º and θ_1 > 88º). Similarly, Figures 3c and 3d suggest that, for rock masses with relatively high discontinuity shear strength, N_{cs} is controlled by the intact rock strength only for rock masses with relatively vertical or horizontal discontinuity sets (θ_1 < 5º and θ_1 > 85º). For all these cases, beyond those discontinuity orientation angles, N_{cs} could drop very significantly with a slight change in θ_1.

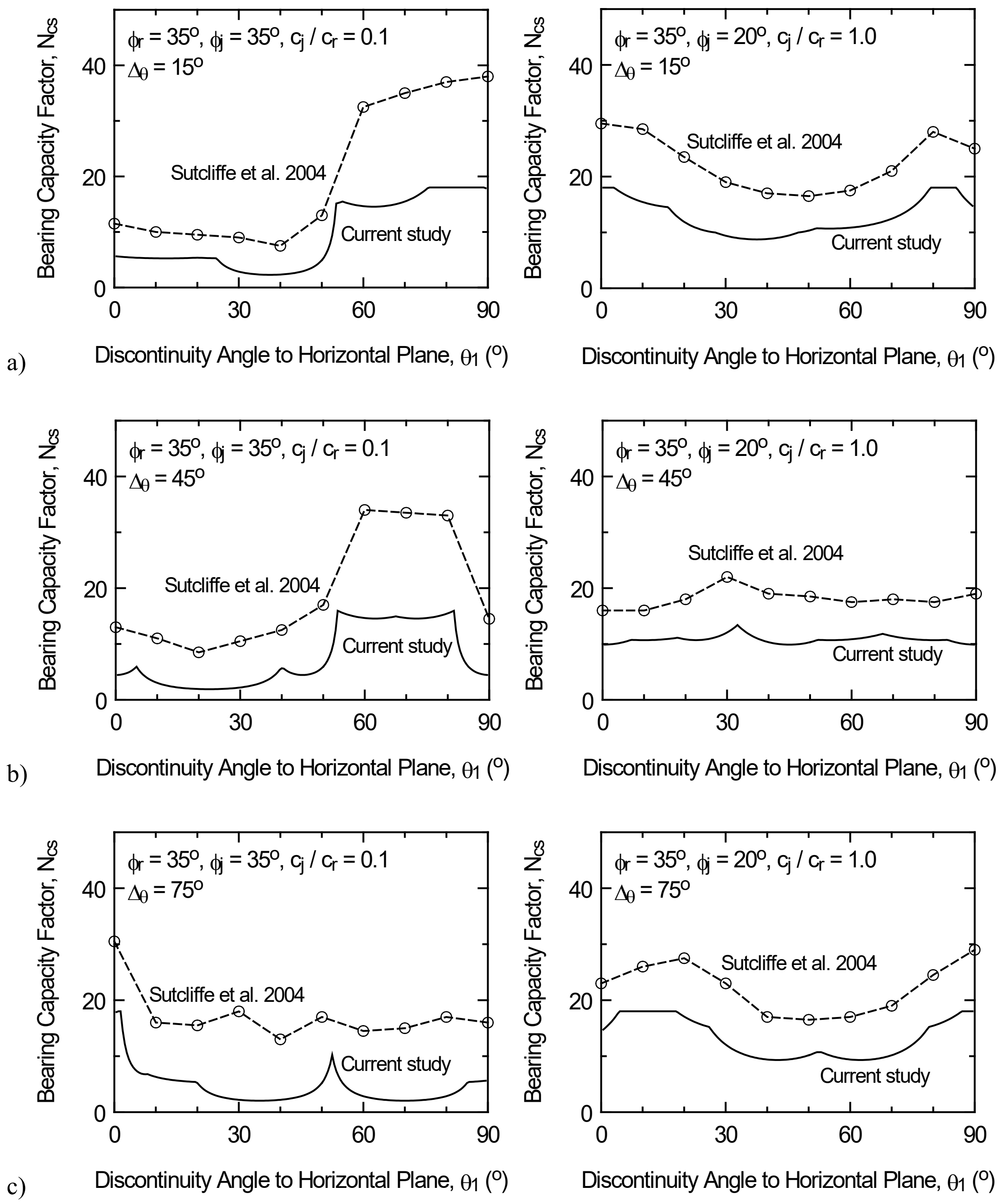

Figure 2. Result comparison of the model of Sutcliffe et al. (2004) and current model for rock masses with two discontinuity sets: a) Δ_θ = 15°, b) Δ_θ = 45°, and c) Δ_θ = 75°.

According to Figure 3, N_{cs} for rock masses with orthogonal discontinuity sets reaches its minimum for θ_1, ranging from about 15° to 75°. It was observed that the range does not change significantly as the discontinuity shear strength changes, meaning that the intact rock friction angle ϕ_r has practically no effect on N_{cs}. However, the discontinuity cohesion c_j/c_r has a more significant effect on N_{cs} such that N_{cs} for rock masses with lower discontinuity strength was lower.

A comparison between Figures 4a and 4b as well as 4c and 4d for rock masses with Δ_θ = 60° showed that a change in ϕ_j altered the general shape of N_{cs} curves, while a change in c_j/c_r affected N_{cs} local peak shapes and values. Furthermore, N_{cs} local peak values are in most cases affected by the intact rock friction angle ϕ_r.

This means that the existence of one vertical and/or horizontal discontinuity set (θ_1 = 0, 30°, and 90°) does not result in high N_{cs}, and no range of these values was controlled solely by the intact rock strength as shown in Figure 4. Also, N_{cs} reaches its minimum in different ranges of θ_1, depending on the discontinuity strength parameters.

It was also observed that a comparison between Figures 5a and 5b as well as 5c and 5d for rock masses with Δ_θ = 30º showed that a change in ϕ_j widened the "plateau" of high N_{cs} values, and an increase in c_j/c_r also widen the "plateau" of high N_{cs} values. Furthermore, N_{cs} local peak values of the "plateau" of high N_{cs} values are affected by ϕ_r.

This simply means that the existence of vertical and/or horizontal discontinuity sets (θ_1 = 0, 60º, and 90º) does not result in high N_{cs}, and no range of these values was controlled solely by the intact rock strength as shown in Figure 5. N_{cs} also reaches its minimum at θ_1 of about 30º, and θ_1 value does not change significantly with the changes in discontinuity shear strength.

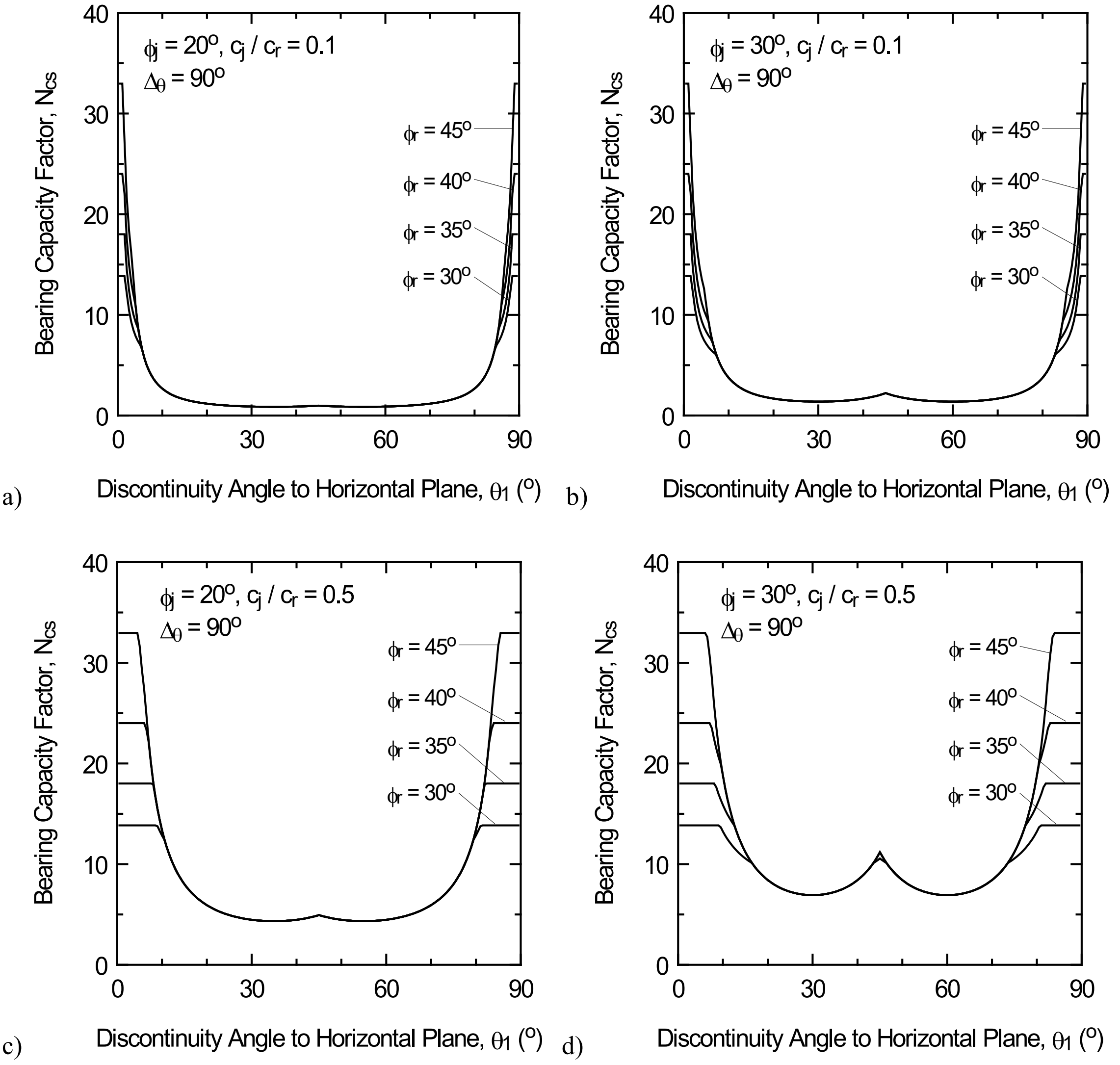

Figure 3. Bearing capacity factor – two discontinuity sets with Δ_θ= 90º.

4 DISCUSSIONS

The results of this model were synthesized to obtain the general trends in the bearing capacity of strip footings on rock masses with two discontinuity sets. It was observed from the cases presented in the twelve figures above that the bearing capacity was not controlled by the intact rock strength, except for a very limited number of cases. The bearing capacity was controlled primarily by the rock structures including the number of discontinuity sets, θ, and Δ_θ, as well as the discontinuity strength such as ϕ_j and c_j/c_r.

The minimum N_{cs} for each combination of ϕ_j, c_j/c_r, and Δ_θ in Figures 3 to 5 were also examined. It is noted that the minimum N_{cs} is the most conservative N_{cs} value for rock strip footing design purposes. Furthermore, the minimum N_{cs} is independent of the intact rock friction angle ϕ_r in all cases, except for the cases in Figure 4d. This minimum N_{cs} in general is a linear function of c_j/c_r, and for example, its value for cases in Figure 4a is linearly correlated to Figure 4c.

The maximum N_{cs} for each combination of ϕ_j, c_j/c_r, and Δ_θ in Figures 4 and 5 were examined, while Figure 3 is independent of ϕ_j and c_j/c_r. It was observed that this maximum N_{cs} is a function of the intact rock friction angle ϕ_r, except for the cases in Figure 4a. However, ϕ_r has an insignificant effect when examined in terms of the ratio of maximum bearing capacity to UCS. The ratio varied from 3.07 to 3.11 for a relatively wide range of ϕ_r in Figure 4b, and varied from 3.83 to 3.87 for cases in Figure 5b. It was also observed that c_j/c_r does not significantly affect the ratio in Figure 4d (c_j/c_r = 0.5), as the ratio varied from 3.47 to 3.77, and does not linearly correlate with the ratio for cases in Figure 4b (c_j/c_r = 0.1).

The ratio of maximum to minimum N_{cs} is generally a function of discontinuity strength, and it is used as an indicator for the sensitivity level of bearing capacity to any variation in θ. The ratios for cases with ϕ_r = 45° in Figures 4b and 4d, indicated a lower and higher discontinuity strengths of 6.63 and 1.49, respectively, meanwhile Figures 5b and 5d, showed a lower and higher discontinuity strengths of 13.35 and 2.94, respectively.

All the exceptions identified above indicated that some rock mass conditions have the potential to result in unexpected rock footing bearing capacities. These exceptions include higher and lower bearing capacity factors in Figure 3 and 4, which highlights the importance of a good characterization process of rock masses when designing rock footings.

The mean and coefficient of variation of the empirical bearing capacity of footings on rock masses in terms of ratio to UCS were 3.46 and 26.8% as reported by Prakoso and Kulhawy (2003), while the minimum and maximum ratios were 2.40 and 5.21, respectively. Although they are not directly comparable and need a more in-depth examination, the empirical ratios were in the same range of maximum bearing capacity ratios. This means that the minimum bearing capacity ratios were too low, and the intact rock bearing capacity ratios were too high to be implemented in the rock footing designs.

5 CONCLUSIONS

This study presented a lower bound model for the bearing capacity of strip footings on rock masses with two discontinuity sets. It is important to note that this model has the ability to handle two discontinuity sets having different cohesion and friction angle values, but it was used to perform a parametric study of footings on those rock masses with the same discontinuity strength. It covered different rock structures and discontinuity strengths, and the results are highlighted below.

- The bearing capacity was primarily controlled by the rock structures including the number of discontinuity sets, θ, and Δ_θ as well as the discontinuity strength, which include ϕ_j and c_j/c_r. This was controlled by the intact rock friction angle ϕ_r for a very limited number of cases.

- The minimum bearing capacity factor was independent of the intact rock friction angle ϕ_r, but it was a linear function of c_j/c_r.
- The bearing capacity factor was also expressed in terms of its ratio to UCS. It was observed that the ratio for the maximum bearing capacity was insignificantly affected by ϕ_r, and not linearly correlated to c_j/c_r.
- The bearing capacity factor for rock masses with low discontinuity strengths tended to be more sensitive to variations in θ.
- The exception to the above four conclusions were that some rock mass conditions lead to unexpected rock footing bearing capacities, indicating that a good rock mass characterization process is always essential.

In addition, the ratio for the maximum bearing capacity was relatively comparable with the empirical bearing capacity of footings on rock masses. However, this comparison requires a more in-depth examination in the future.

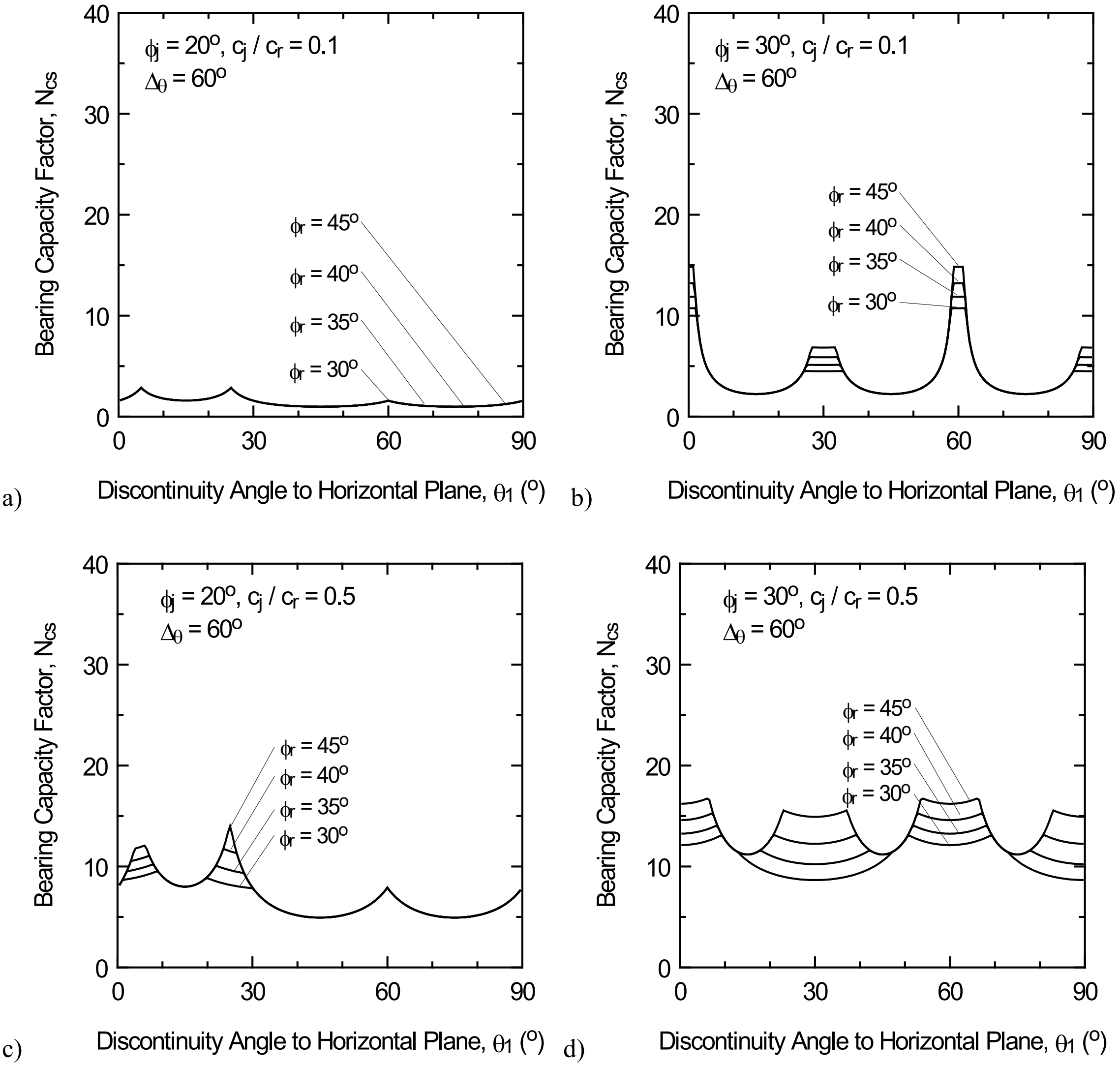

Figure 4. Bearing capacity factor – two discontinuity sets with Δ_θ= 60°.

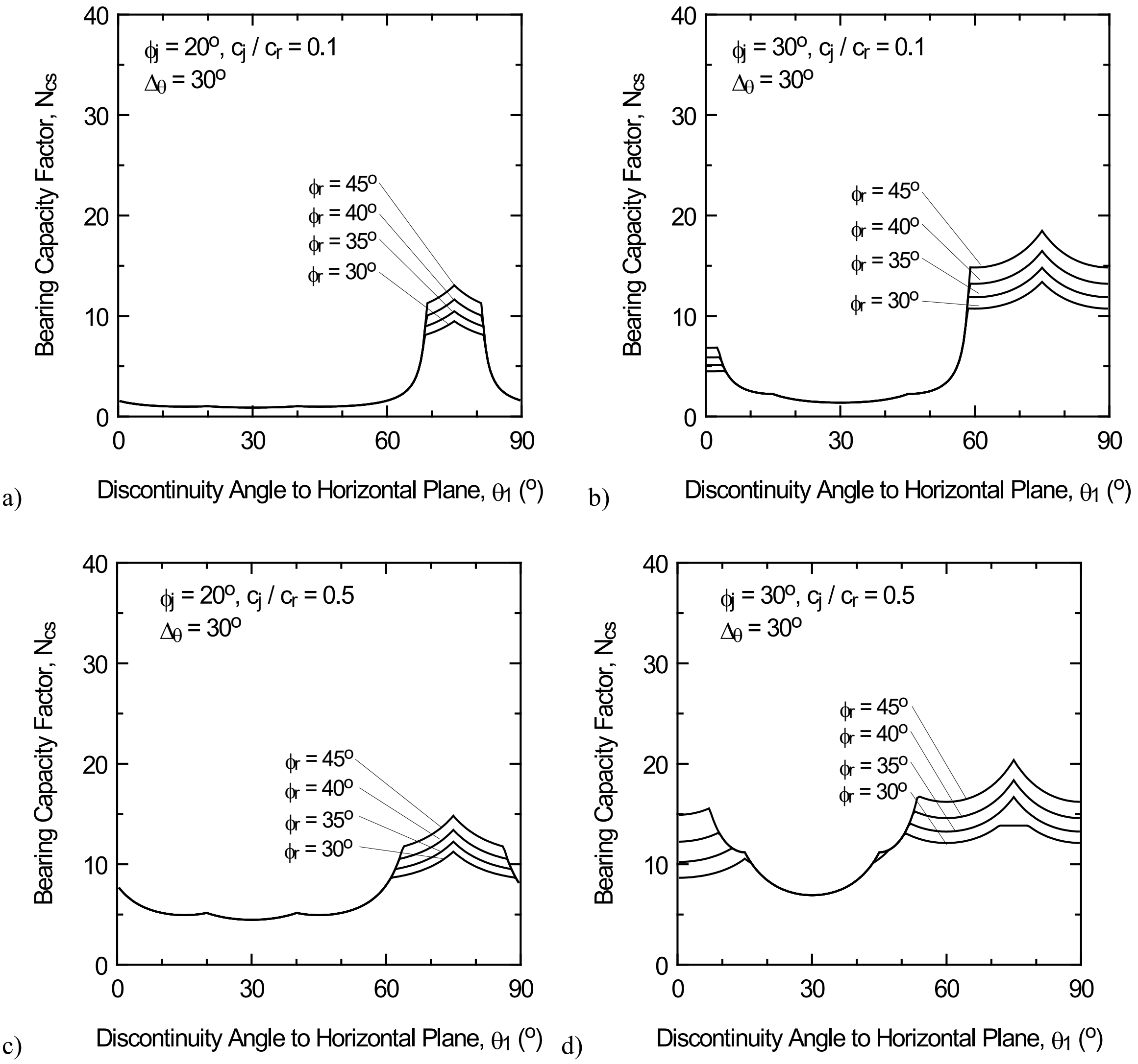

Figure 5. Bearing capacity factor – two discontinuity sets with Δ_θ= 30º.

DISCLAIMER

The author declares no conflict of interest.

AVAILABILITY OF DATA AND MATERIALS

All data and materials have been presented in this study.

ACKNOWLEDGMENTS

The author is in debt to the late Professor Fred H. Kulhawy of Cornell University for his great insights in foundation engineering.

REFERENCES

Alehossein, H., Carter, J.P. & Booker, J.R., 1992. Finite element analysis of rigid footings on jointed rock, *3rd International Conference on Computational Plasticity*, Barcelona, Spain.

Bell, A.L., 1915. Lateral pressure and resistance of clay, and the supporting power of clay foundations. *Proceedings of Institution of Civil Engineers*, 199.

Booker, J.R., 1991. Analytical methods in geomechanics, 7th *International Conference on Computational Methods and Advances in Geomechanics*, Cairns, Australia.

Chakraborty, M., Kumar, J., 2015, Bearing capacity of circular footings over rock mass by using axisymmetric quasi lower bound finite element limit analysis, *Computers and Geotechnics*, 70.

Davis, E.H., 1980. A note on some plasticity solutions relevant to the bearing capacity of rock and fissured clay, *International Conference Structural Foundations on Rock*, Sydney, Australia.

Galindo, R.A., Serrano, A., Olalla, C., 2017, Ultimate bearing capacity of rock masses based on modified Mohr-Coulomb strength criterion, *International Journal of Rock Mechanics and Mining Sciences*, 93.

Goodman, R.E., 1980. *Introduction to Rock Mechanics*. New York: Wiley.

Hoek, E., 2007, *Practical Rock Engineering*. [Online] Available at: https://www.rocscience.com/learning/hoeks-corner [Accessed 4 June 2022].

Merifield, R.S., Lyamin, A. V., Sloan, S. W., 2006, Limit analysis solutions for the bearing capacity of rock masses using the generalised Hoek–Brown criterion, *International Journal of Rock Mechanics and Mining Sciences*, 43(6).

Prakoso, W.A. & Kulhawy, F.H., 2003. Reliability-based design for rock footings, *International Workshop on Limit State Design in Geotechnical Engineering Practice*, Cambridge, USA.

Prakoso, W.A. & Kulhawy, F.H., 2004a. Bearing capacity of strip footings on jointed rock masses, *ASCE J. Geotechnical & Geoenvironmental Engineering*, 130(12).

Prakoso, W.A. & Kulhawy, F.H., 2004b. Variability of rock mass engineering properties. *15th Southeast Asian Geotech Conference*, Bangkok, Thailand.

Prakoso, W.A., Kulhawy, F.H., 2006, Capacity of foundations on discontinuous rock, *41st U.S. Symposium Rock Mechanics*, Golden, USA.

Prakoso, W.A. & Kulhawy, F.H., 2011. Some observations on reliability-based design of rock footings, *Geotechnical Risk Assessment and Management*. Atlanta, USA, ASCE GSP 224.

Salari-Rad H., Mohitazar, M., Dizadji, M.R., 2013, Distinct element simulation of ultimate bearing capacity in jointed rock foundations, *Arabian Journal of Geosciences*, 6(11).

Sutcliffe D.J., Yu H.S., Sloan S.W., 2004, Lower bound solutions for bearing capacity of jointed rock, *Computers and Geotechnics*, 31.

Yu, H.S. & Sloan, S.W., 1994. Bearing capacity of jointed rock, *8th International Conference on Computational Methods and Advances in Geomechanics*. Morgantown, USA.

APPENDIX

The procedure proposed by Prakoso and Kulhawy (2004a) is extended herein for two discontinuity sets having different discontinuity cohesion and friction angle values.

1) To calculate the strength of Zone I.

a) Calculate the strength of rock material with $\sigma_3 = 0$.

$$\sigma_{1r} = 2 \cdot c_r \cdot \tan(45° + \phi_r/2) \quad \text{(A1)}$$

b) Transform the discontinuity angles θ_1 and θ_2 for Zone I (θ_1 = 0 to 90°).

$$\theta_1^* = 90° - \theta_1 \quad \text{(A2a)}$$

For $\theta_1^* \geq \Delta_\theta$

$$\theta_2^* = \theta_1^* - \Delta_\theta \quad \text{(A2b)}$$

For $\theta_1^* < \Delta_\theta$ $\qquad \theta_2^* = \Delta_\theta - \theta_1^*$ (A2c)

Transform the discontinuity angles θ_1 and θ_2 for Zone I [θ_1 = 90° to (180° – Δ_θ)].

$$\theta_1^* = \theta_1 - 90° \tag{A2d}$$

For $\theta_1^* + \Delta_\theta \leq 90°$ $\qquad \theta_2^* = \theta_1^* + \Delta_\theta$ (A2e)

For $\theta_1^* + \Delta_\theta > 90°$ $\qquad \theta_2^* = 180 - \theta_1^* - \Delta_\theta$ (A2f)

c) Calculate the strength of discontinuities for θ_1 = 0 to 90°. Eq. A1 is used to satisfy the no tension requirement of the first discontinuity set, $\theta_1^* \leq \phi_{j1}$ while the equation below is used for $\theta_1^* > \phi_{j1}$

$$\sigma_{1j1} = \frac{2 \cdot c_{j1}}{(1 - tan\phi_{j1}/tan\theta_1^*) \cdot sin(2\theta_1^*)} \tag{A3a}$$

Eq. A1 is also used to satisfy the no tension requirement for the second discontinuity set, $\theta_2^* \leq \phi_{j2}$, while the equation below was used for $\theta_2^* > \phi_{j2}$:

$$\sigma_{1j2} = \frac{2 \cdot c_{j2}}{(1 - tan\phi_{j2}/tan\theta_2^*) \cdot sin(2\theta_2^*)} \tag{A3b}$$

d) Calculate the strength of Zone I.

$$\sigma_{1-I} = \min(\sigma_{1r}, \sigma_{1j1}, \sigma_{1j2}) \tag{A4}$$

2) To calculate the strength of Zone II.

a) Establish the confining stress.

$$\sigma_{3-II} = \sigma_{1-I} \tag{A5}$$

b) Calculate the strength of rock material.

$$\sigma_{1r} = \sigma_{3-II} \cdot tan^2(45° + \phi_r/2) + 2 \cdot c_r \cdot \tan(45° + \phi_r/2) \tag{A6}$$

c) Transform the discontinuity angle θ_2 for Zone II, whereθ_1 = 0 to 90°.

$$\theta_1^{**} = \theta_1 \tag{A7a}$$

For $\theta_1^{**} + \Delta_\theta \leq 90°$ $\qquad \theta_2^{**} = \theta_1^{**} + \Delta_\theta$ (A7b)

For $\theta_1^{**} + \Delta_\theta > 90°$ $\qquad \theta_2^{**} = 180° - \theta_1^{**} - \Delta_\theta$ (A7c)

Transform the discontinuity angle θ_2 for Zone II and [θ_1 = 90° to (180° – Δ_θ)].

$$\theta_1^{**} = 180° - \theta_1 \tag{A7d}$$

For $\theta_1^{**} \geq \Delta_\theta$ $\qquad \theta_2^{**} = \theta_1^{**} - \Delta_\theta$ (A7e)

For $\theta_1^{**} < \Delta_\theta$ $\qquad \theta_2^{**} = \Delta_\theta - \theta_1^{**}$ (A7f)

d) Calculate the strength of discontinuities for θ_1 = 0 to 90°. Eq. A6 is used to satisfy the no tension requirement for the first discontinuity set, $\theta_1^{**} \leq \phi_{j1}$, and, for $\theta_1^{**} > \phi_{j1}$, the following equation is used:

$$\sigma_{1j1} = \sigma_{3-II} + \frac{2 \cdot c_{j1} + 2 \cdot \sigma_{3-II} \cdot tan\phi_{j1}}{(1 - tan\phi_{j1}/tan\theta_1^{**}) \cdot sin(2\theta_1^{**})} \tag{A8a}$$

Eq. A6 is used to satisfy the no tension requirement for the second discontinuity set, $\theta_2^{**} \leq \phi_{j2}$, while for $\theta_2^{**} > \phi_{j2}$, the following equation is used:

$$\sigma_{1j2} = \sigma_{3-II} + \frac{2 \cdot c_{j2} + 2 \cdot \sigma_{3-II} \cdot tan\phi_{j2}}{(1 - tan\phi_{j2}/tan\theta_2^{**}) \cdot sin(2\theta_2^{**})} \quad \text{(A8a)}$$

e) Calculate the strength of Zone II (end bearing capacity).

$$q_{ult} = \sigma_{1-II} = \min(\sigma_{1r}, \sigma_{1j1}, \sigma_{1j2}) \quad \text{(A9)}$$